Supplementary Information

Moderately clustered gold nanoparticles preserved in in-situ polymerized hydrogels towards facile SERS sensing

Hikaru Namigata[1,], Kanako Watanabe[1], Tom A. J. Welling[1,2], Keishi Suga[1], Daisuke Nagao[1,]**

1 Department of Chemical Engineering, Tohoku University, 6-6-07 Aoba, Aramaki-aza, Aoba-ku, Sendai, Miyagi, 980-8579, Japan

2 Frontier Research Institute for Interdisciplinary Sciences, Tohoku University, Sendai, Miyagi, 980-8579, Japan

*E-mail: h.namigata@tohoku.ac.jp (H.N.), dnagao@tohoku.ac.jp, (D.N.)

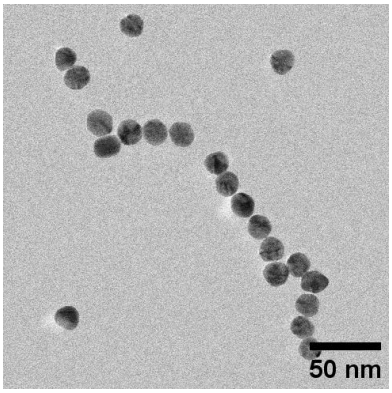

Figure S1. TEM image of AuNPs. The volume-averaged diameter (d_V) and coefficient of variation (Cv) were 16 nm and 6.0%, respectively.

The volume-averaged diameter d_V and coefficient of variation Cv, or polydispersity, of the synthesized particles were calculated using the following equations[1–3]:

$$d_V = \left(\sum n_i d_i^3 / \sum n_i\right)^{1/3}, \quad \text{(S1)}$$

$$C_V = \frac{\left[\sum\{d_i - (\sum n_i d_i / \sum n_i)\}^2\right]^{1/2}}{\sum n_i d_i / \sum n_i} \times 100\ , \quad \text{(S2)}$$

where n_i is the number of particles with diameter d_i.More than 200 particles were measured to determine d_V.

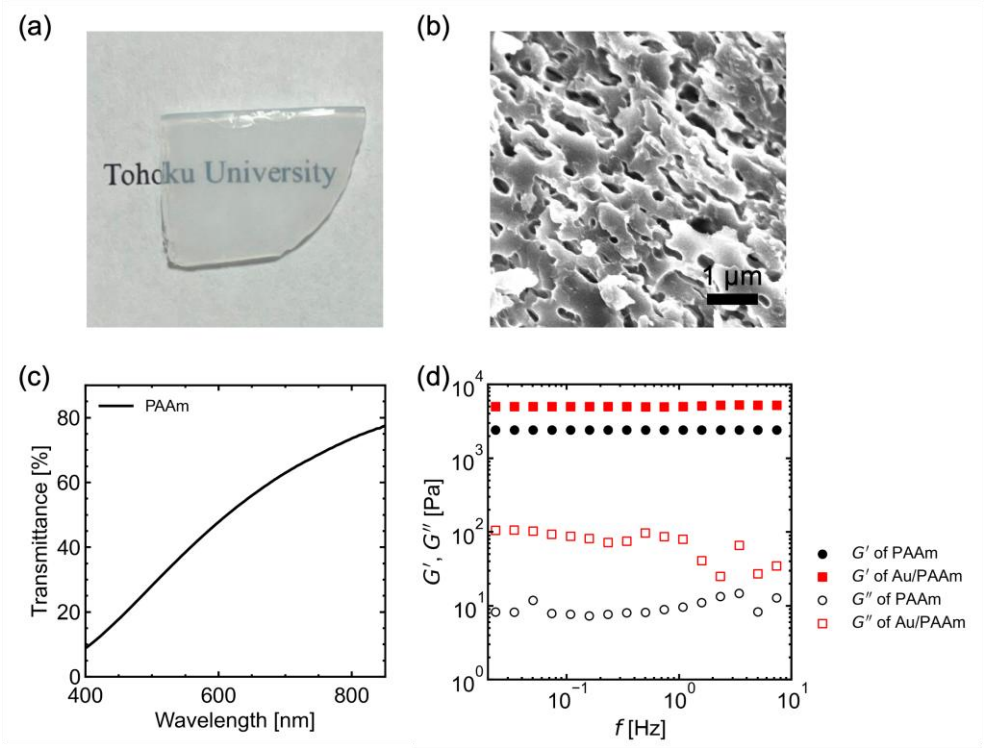

Figure S2. (a) Digital photograph of a PAAm hydrogel film, (b) SEM image of a PAAm hydrogel film, (c) Transmittance spectrum of a PAAm hydrogel film, and (d) storage modulus (*G'*) and loss modulus (*G''*) of PAAm (black plots) and Au/PAAm (red plots) as a function of angular frequency, measured at 25°C using a rotational rheometer (RheoStress 6000, HAAKE).

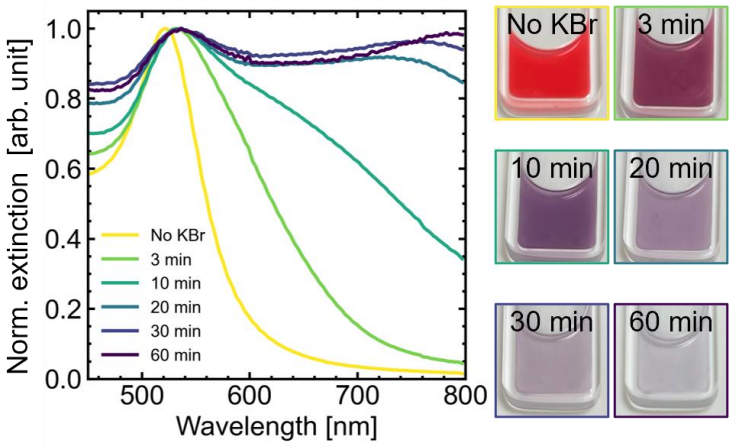

Figure S3. (left) Extinction spectra and (right) digital photographs of AuNPs in aqueous solution of hydrogel precursors with 1.0 M KBr.

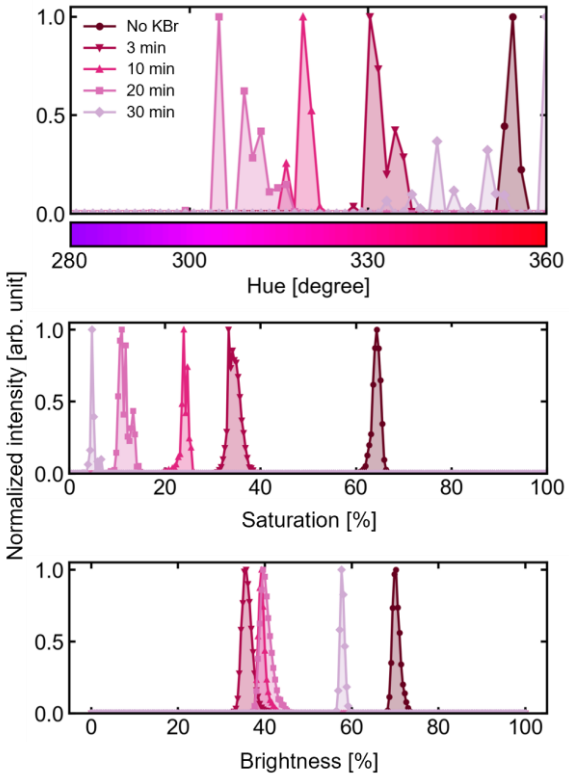

Figure S4. Hue, saturation, and brightness histograms of AuNPs/PAAm, AuNCs/PAAm-3, -10, -20, and -30 calculated from Figure 1(a) using ImageJ Fiji software.

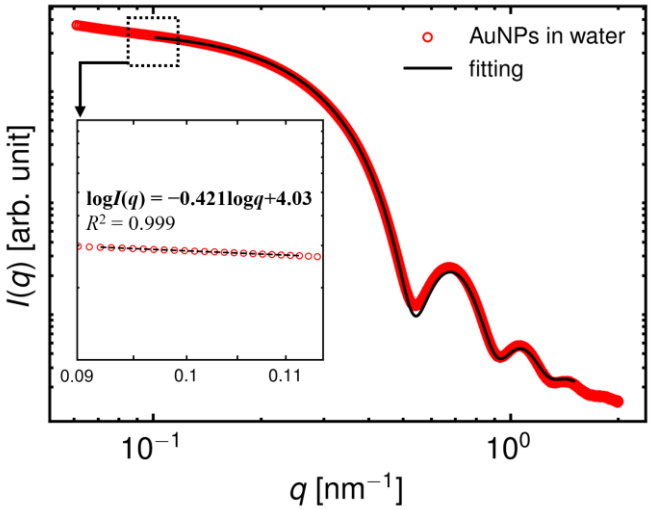

Figure S5. 1D SAXS profile of AuNPs in water and a fitting curve calculated assuming a sphere model using SasView software (v.6.0.0). Fitting range was 0.1–1.5 nm^{-1}, and the radius and polydispersity were 8.2 nm and 0.08, respectively. The inset figure shows a linear trendline of the profile, which was calculated using the least squares method.

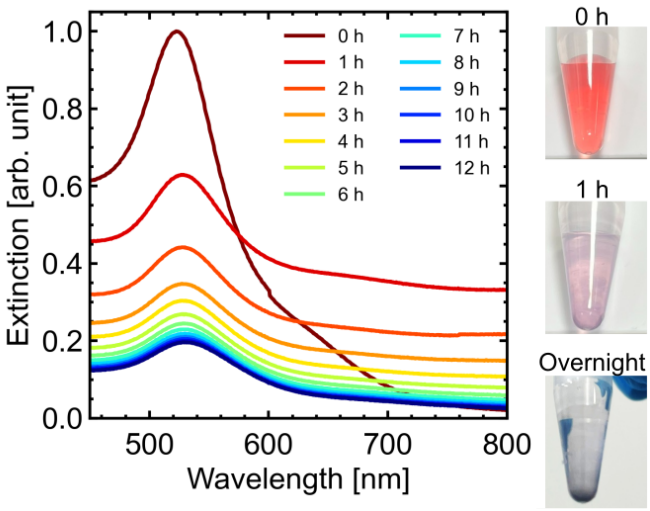

Figure S6. Extinction spectra and digital photographs of AuNPs in a 1.0 M KBr aqueous solution taken at various timings after the electrolyte addition. The increase in extinction intensity from 0to 1 h is due to generation of nanoparticle clusters. On the other hand, the decrease in extinction intensity over time (2–12 h) is due to the sedimentation of large aggregates, resulting in a clear supernatant as shown in the photographs.

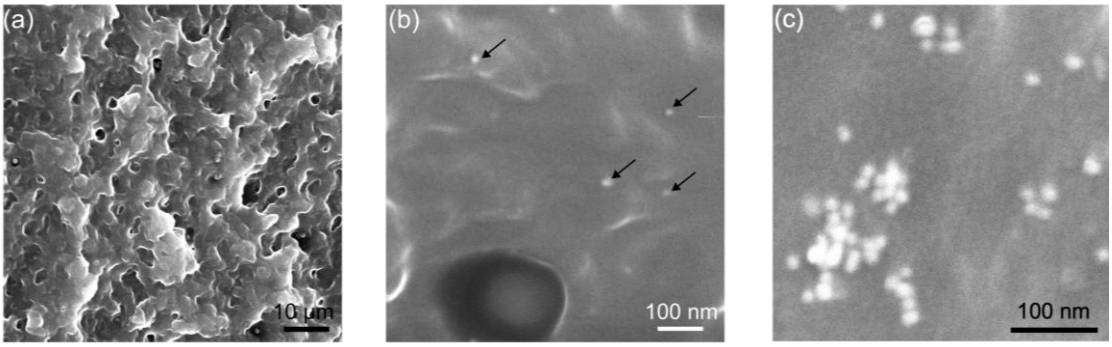

Figure S7. SEM images of AuNPs/PAAm films: (a) low and (b) high magnifications. Black arrows in (b) point AuNPs. (c) SEM image of a AuNCs/PAAm-20 film.

Absorption property of AuNCs with varied interparticle distances

A finite-element method calculation was performed using COMSOL Multiphysics® (ver. 5.6). Since the hydrodynamic diameter of AuNCs-3 was approximately 3 times larger than that of AuNPs, an octahedral structure was employed as a finite-element model for simplicity. This is because an octahedral structure can manage both a minimal number of component particles and maximal symmetry. Figure S8 shows the constructed 3D model. Seven spherical AuNPs with a radius of 8 nm were arranged inside a spherical space with a radius 12 times the radius of AuNPs. The surface distance of neighboring AuNPs, *h*, ranged from 0.5 to 20 nm. The spherical space was filled with water. The perfect matched layer (PML) that absorb outgoing waves was applied to the outer surface of the space. The incident light that was polarized in the *y* direction entered from the *z* direction. The absorption cross section was calculated according to the previous studies [4,5].

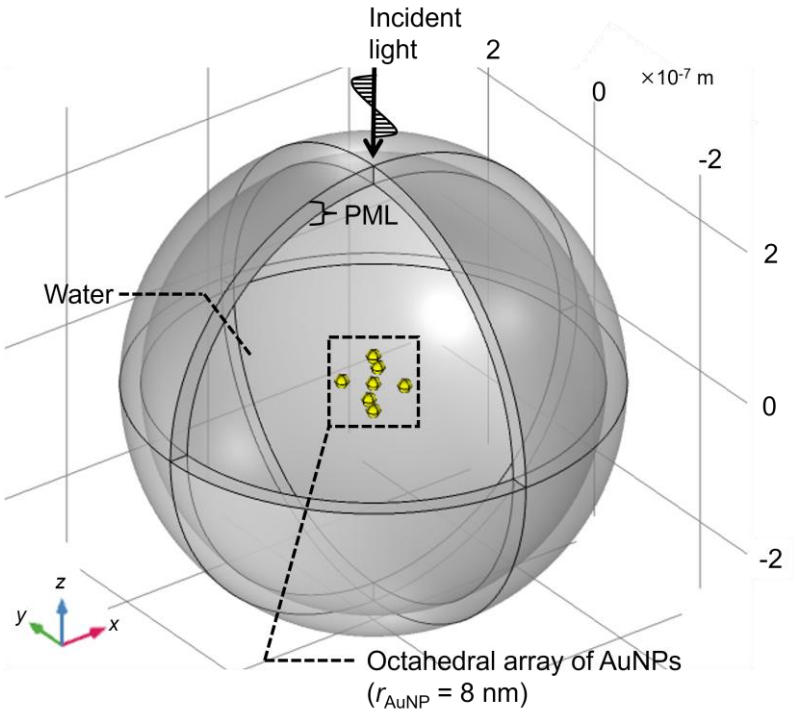

Figure S8. Schematic illustration of the finite-element model for a gold nanoparticle cluster.

The Absorption cross section spectra calculated with varied *h* were shown in Figure S9.

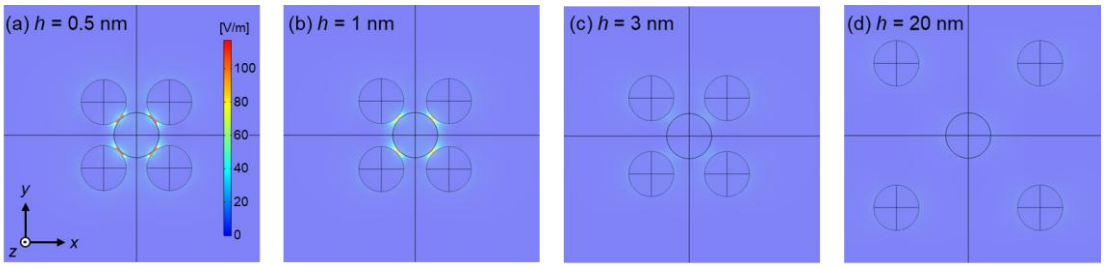

Figure S9. Electric field mappings observed from a direction parallel to the z axis: h = 0.5 nm (a), 1 nm (b), 3 nm (c), and 20 nm (d). The electric fields were excited with optimized wavelengths (λ_{max}).

From the calculation results, hotspots clearly appeared when $h \geq 3$ nm, and λ_{max} was redshifted with decreasing h. Those calculations showed that the absorption capacity of AuNCs for a longer wavelength region is improved when the component AuNPs approached, even if the number of component particles is consistent.

Estimation of the limit of detection and quantification

Limit of detection (LOD) and limit of quantification (LOQ) can be theoretically estimated using the blank measurements of Raman (or SERS) spectra. Statistically, LOD is defined as a value that adding 3 times σ (*i.e.*, standard deviation) to the average of the measured background values. As well as this, LOQ is defined as a value obtained by adding 10σ to the average of the background.

Here, blank measurements were performed with PAAm films for 10 times and with the exposure time of 20 or 40 seconds, which were for PMBA or creatinine, respectively. For PMBA and creatinine, Raman signal intensity at 1585 cm^{-1} or 680 cm^{-1} was used to calculate 3σ- and 10σ-criteria. Averaged blank measurement plots are shown in Figure S11. By considering the trendline of AuNCs/PAAm films (Figure 4(c) and Figure 5(b)), LOD and LOQ can be estimated.

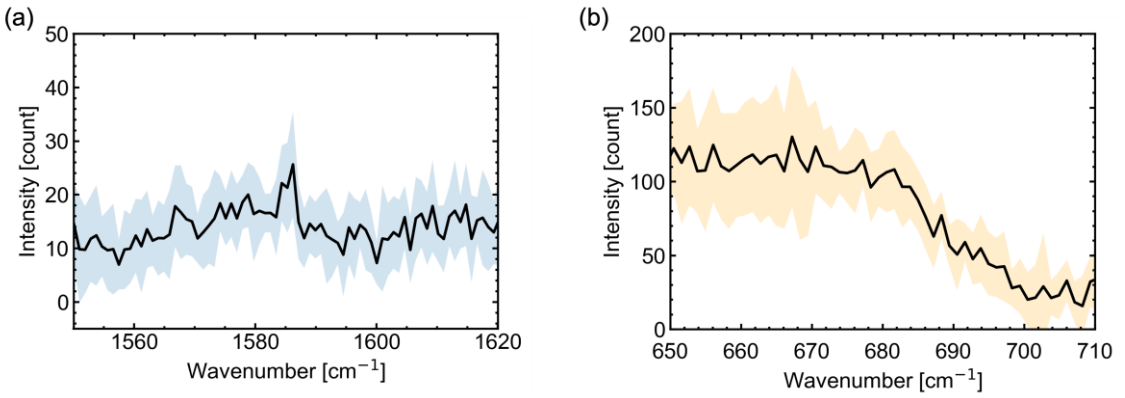

Figure S10. Raman spectra of PAAm films with the exposure time of (a) 20 s and (b) 40 s. Translucent range shows the standard deviation of the signal intensities.

Peak attribution of a PAAm film in Raman measurements

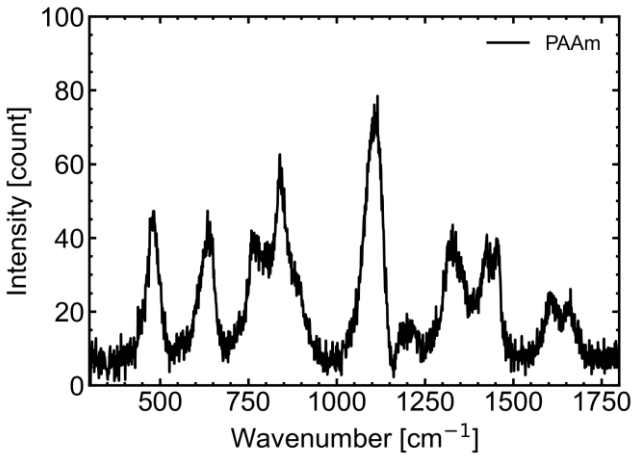

Figure S11. Raman spectrum of a PAAm film.

Table S2. Raman peak attribution of a PAAm hydrogel.

Peaks in Figure S8 [cm^{-1}]	Peaks in literature	Attribution
482	480[6]	Indicating the presence of polymeric chains
634	~630[7]	Rocking of C–C
770	770[6]	Rocking of –$(CH_2)_n$–
838	~850[7]	Bending of C–H
1108	1100[6]	Indicating tans conformational states
1218, 1424, 1608	1280, 1430, 1615[6]	Indicating gauche conformational states
1327, 1454	1325, 1455[6]	Indicating trans conformational states
1662	~1650[7]	Stretching of C=C

References

[1] M. Okubo, T. Nakagawa, *Colloid Polymer Sci*., **1992***, 270*, 853.

[2] V. Hwang, A. B. Stephenson, S. Barkley, S. Brandt, M. Xiao, J. Aizenberg, V. N. Manoharan, *Proc Natl Acad Sci U S A* **2021**, *118*, e2015551118.

[3] K. Watanabe, R. Fujinuma, H. Aizawa, H. Namigata, T. A. J. Welling, K. Suga, D. Nagao, *Microporous and Mesoporous Materials* **2024**, *379*, 113274.

[4] A. García-Etxarri, R. Gómez-Medina, L. S. Froufe-Pérez, C. López, L. Chantada, F. Scheffold, J. Aizpurua, M. Nieto-Vesperinas, J. J. Sáenz, *Opt Express* **2011**, *19*, 4815.

[5] M. Hasegawa, K. Watanabe, H. Namigata, T. A. J. Welling, K. Suga, D. Nagao, *J Colloid Interface Sci* **2023**, *633*, 226.

[6] N. G. Golubeva, A. O. Velikanov, *J Appl Spectrosc* **1990**, *53*, 1290.

[7] B. B. Sharma, C. Murli, S. M. Sharma, *Journal of Raman Spectroscopy* **2013**, *44*, 785.